The Oxidative Addition of Iodomethane to Thioacetylacetonatocarbonylphosphine-rhodium(I) Complexes

J. G. LEIPOLDT, S. S. BASSON and L. J. BOTHA

Department of Chemistry, University of the Orange Free State, Bloemfontein (South Africa)

(Received July 4, 1989)

Abstract

The oxidative addition of iodomethane to $[Rh(Sacac)(CO)(PX_3)]$, where X = phenyl, *p*-chlorophenyl, *p*-methoxyphenyl and cyclohexyl has been found to follow second-order kinetics and give only the acylrhodium(III) complex as product. The reactions proceed through an alkylrhodium(III) intermediate. The reaction rate is influenced by the polarity of the solvent and by the electronic and steric properties of the phosphine ligand.

Introduction

We have recently reported on the oxidative addition of iodomethane to $[Rh(LL)(CO)(PX_3)]$ and $[Rh(LL)(P(OPh)_3)_2]$ complexes [1–4] (LL = β-diketones and cupferron and X = phenyl, *p*-chlorophenyl and *p*-methoxyphenyl). Although the results were in favour of an ionic S_N2 mechanism, a high pressure kinetic study showed that a concerted three-center *cis*-addition mechanism is a viable alternative [5]. The latter mechanism is a well-known alternative especially in the case of homonuclear addend-molecules like dihydrogen [6]. In the case of the β-diketone complexes, [Rh(β-diketone)(CO)(PX_3)], the final alkyl complexes formed via an ionic intermediate and the acyl complex [2]. Both these intermediates were observed by means of IR time scans. In the case of the cupferron complex we isolated the alkyl complex and observed that the acyl complex is not an intermediate as in the case of the β-diketone complexes but is formed slowly from the alkyl complexes [3]. It is thus clear that the reactions mechanism is influenced by the nature of the bidentate ligand.

The formation of rhodium acyl species is important in a variety of homogeneous catalyzed processes such as in the Monsanto process for the synthesis of acetic acid [7]. In many systems the acylrhodium intermediates have been established by observation of the characteristic carbonyl stretching frequency at about 1700 cm^{-1}. In some cases the acyl complex is the final reaction product between a Rh(I) complex and CH_3I.

The final isomer that is formed during the oxidative addition of CH_3I (acyl or alkyl) should depend on the nucleophilicity of the ligands in the metal complex. In the case of $[Rh(LL)(CO)(PX_3)]$ complexes it is noticeable that the acyl complex is formed if one or both of the donor atoms of the bidentate ligand is a sulphur atom [8]. For LL = β-diketones [1, 2] cupferron [3] or 8-hydroxyquinoline [9] the final product is the alkyl complex. An explanation for this behaviour may be found in the capability of the other donor atoms to stabilize the Rh(III)–acyl bond. It appears that the acyl complex is stabilized (relative to the alkyl complex) by more nucleophilic donor atoms (like a sulphur atom) of the bidentate ligand. To further understand the role of different donor atoms of the bidentate ligand in complexes of the type $[Rh(LL)(CO)(PX_3)]$ the oxidative addition of CH_3I to [Rh(Sacac)(CO)-(PX_3)] complexes (HSacac = thioacetylacetone) was investigated.

Experimental

Syntheses

[Rh(Sacac)(CO)$_2$]

A solution of $[Rh_2Cl_2(CO)_4]$ was prepared by refluxing a solution of 0.25 g of $RhCl_3 \cdot 3H_2O$ in 30 cm^3 dimethylformamide for approximately 30 min [10]. An equivalent amount of thioacetylacetone (HSacac) (synthesized as described in the literature [11]) was added to the resulting yellow solution. About 300 cm^3 cold water was added to this solution to precipitate the $[Rh(Sacac)(CO)_2]$. The red precipitate was removed by centrifuging and washed twice with cold water. [Rh(Sacac)-$(CO)_2$] was recrystallized from methanol. The ^1H NMR and infrared data are listed in Table 1.

[Rh(Sacac)(CO)(PX$_3$)] complexes

The $[Rh(Sacac)(CO)(PX_3)]$ complexes (X = C_6H_5, *p*-$CH_3OC_6H_4$, *p*-ClC_6H_4 and C_6H_{11}) were prepared by adding an equivalent amount of the phosphine to a solution of 0.1 g of $[Rh(Sacac)(CO)_2]$ in 20 cm^3 acetone. The solution was evaporated to give

0020-1693/90/$3.50

TABLE 1. ^{1}H NMR (in $CDCl_3$) and ν(CO) (KBr disks) data for the different complexes

Compound	δ (ppm)				ν(CO) (cm^{-1})
	$CH_3C(O)$	$CH_3C(S)$	–CH–	$COCH_3$	
HSacac	2.13	2.34	6.29		
[Rh(Sacac)$(CO)_2$]	2.25	2.52	6.73		1966, 2064
[Rh(Sacac)(CO)(P(*p*-$CH_3OC_6H_4)_3$]	1.70	2.49	6.52		1968
[Rh(Sacac)(CO)(PPh_3)]	1.67	2.52	6.56		1978
[Rh(Sacac)(CO)(P(*p*-$ClC_6H_4)_3$)]	1.72	2.53	6.58		1981
[Rh(Sacac)(CO)(P($C_6H_{11})_3$]	[a]	2.48	6.59		1952
[Rh(Sacac)($COCH_3$)(I)(P(*p*-$CH_3COC_6H_4)_3$)]	2.18	2.34	6.52	2.67	1717
[Rh(Sacac)($COCH_3$)(I)(PPh_3)]	2.18	2.37	6.52	2.69	1716
[Rh(Sacac)($COCH_3$)(I)(P(*p*-$ClC_6H_4)_3$)]	2.22	2.40	6.58	2.64	1719

[a]Overlap with $-C_6H_{11}$ signals.

a fine yellow powder. The powder was dissolved in a minimum of cold acetone (about 5 cm^3) and 10 cm^3 n-hexane was added to this solution. The solution was allowed to evaporate at room temperature. A fine yellow crystalline precipitate was obtained for all the phosphines. The ^{1}H NMR and infrared data are given in Table 1.

[Rh(Sacac)($COCH_3$)(I)(PX_3)] complexes

CH_3I (2 g) was added to a solution of 0.07 g of [Rh(Sacac)(CO)(PX_3)] in 13 cm^3 of acetone. The mixture was sealed to prevent evaporation of the iodomethane. The reaction progress was monitored by means of infrared spectra (decrease of the Rh(I)–CO peak). n-Hexane (15 cm^3) was added to the solution after complete disappearance of the Rh(I)–CO peak (about 60 min). The solution was allowed to evaporate at room temperature. A fine orange powder was obtained for all the phosphines. The ^{1}H NMR and infrared data are listed in Table 1. *Anal.* for the triphenyl phosphine complex, [Rh(Sacac)($COCH_3$)(I)(PPh_3)]: calc. for $C_{25}H_{25}O_2SPIRh$: C, 46.17; H, 3.86; O, 4.94; S, 4.93; P, 4.76; I, 19.52; Rh, 15.82. Found: C, 46.76; H, 4.07; O, 5.27; S, 4.64; P, 4.67; I, 19.40; Rh, 15.30%.

Kinetics

All the infrared measurements were done on a Hitachi model 270-50 spectrophotometer with a wave number accuracy of 2 cm^{-1} in the region employed. The kinetic measurements were performed in a thermostated cell (±0.1 °C) with a 0.5 mm pathlength and NaCl windows. The reaction progress was monitored in the infrared region from the disappearance of the Rh(I)–CO peak as well as the formation of the Rh(III)–acyl's carbonyl peak. The concentration of the Rh(I) complexes was about 2×10^{-2} mol dm^{-3} in all the cases.

The visible spectrophotometric measurements were performed on a Hitachi model 150-20 spectrophotometer equipped with a thermostated (±0.1 °C) cell holder. The concentration of the different Rh(I) complexes was about 2×10^{-4} mol dm^{-3} for all the kinetic measurements.

The concentration of the iodomethane was varied between 0.1 and 1.0 mol dm^{-3} to ensure good pseudo-first-order plots of $\ln(|A_\infty - A_t|)$ versus time. All the calculations were performed on a Univac 1100 computer using a non-linear least-squares program.

Results and Discussion

The two methyl groups in [Rh(Sacac)$(CO)_2$] are not chemically equivalent. The ^{1}H NMR spectrum therefore shows two methyl signals, singlets at δ = 2.25 and 2.52 ppm ($(CD_3)_2CO$), for the bidentate ligand Sacac-methyl protons. The assignment (see Table 1) is according to that of HSacac [12] which is justified since the two metal-bonded carbonyl groups should have an equivalent effect on the two methyl groups.

The ^{1}H NMR spectra of the [Rh(Sacac)(CO)(PX_3)] complexes also show two singlet methyl signals. The results of the crystal structure determination of [Rh(Sacac)(CO)(PPh_3)] [13] as well as nuclear Overhauser effects were used to assign these signals. The crystal structure determination of [Rh(Sacac)(CO)(PPh_3)] showed that only the carbonyl group *trans* to the sulphur atom in [Rh(Sacac)$(CO)_2$] was substituted by PPh_3 indicating that the sulphur atom of Sacac has a larger *trans* influence than the oxygen atom. The phenyl protons should thus have the largest association with the methyl protons nearest to the oxygen atom of Sacac. The methyl signal at δ = 1.67 ppm showed the largest association with the phenyl protons and was thus accordingly assigned to the $CH_3C(O)$ group, see Table 1. The assignment of the methyl signals for the other complexes was done in the same way.

The microanalysis of the oxidative addition product of the reaction between [Rh(Sacac)(CO)-(PPh_3)] and CH_3I confirmed the expected composition, i.e. $C_{25}H_{25}O_2SPIRh$. The ^1H NMR spectrum shows three singlets indicating an extra methyl group due to the oxidative addition of CH_3I. Since a metal bonded CH_3 group is expected to couple with both the rhodium and phosphorous atoms (as was found in [Rh(cupf)(CO)(CH_3)(I)(PPh_3)] [3] and [Rh(acac)(CH_3)(I)($P(OPh)_3$)$_2$] [4]) the observed singlet points to methyl migration (carbonyl insertion) resulting in the acyl complex [Rh(Sacac)($COCH_3$)(I)(PPh_3)]. The assignment of the methyl signal of the acyl group (see Table 1) is based on the observation that the methine hydrogen atom shows an equal association with the methyl signals at $\delta = 2.18$ and 2.34 ppm and no association with the methyl signal at $\delta = 2.69$ ppm while the assignment of the methyl signals of the chelate ring ($CH_3C(O)$ and $CH_3C(S)$ groups) is based on the fact that the methyl signals of the $CH_3C(S)$ group was shifted to a lower field relative to those of the $CH_3C(O)$ group in the other complexes, see Table 1. The different phosphines do not have a large influence on the position of the different methyl and methane hydrogen signals.

The carbonyl stretching vibrations, ν(CO), in the vicinity of 1720 cm^{-1} also verify that the acyl complex is the final oxidative addition product in all the cases. No absorption in the infrared region between 2000 and 2100 cm^{-1} was observed as was the case for other Rh(III)–CO complexes such as [Rh(acac)(CO)(CH_3)(I)(PX_3)] [2] and [Rh(cupf)-(CO)(CH_3)(I)(PX_3)] [3].

All the [Rh(Sacac)(CO)(PX_3)] complexes reported here are stable in the solvents used for this investigation, i.e. toluene, ethylacetate, chlorobenzene, acetone, 1,2-dichloroethane and acetonitrile. On the other hand, UV–Vis time scans (340–500 nm) for a methanol solution of [Rh-(Sacac)(CO)(PPh_3)] showed a slow decomposition with rate constant $1.17(4) \times 10^{-5}$ s^{-1} at 25 °C. The absorption changes in the afore-mentioned solvents were however negligible during a period of up to 3 h.

Preliminary investigation (by means of infrared time scans in the region 1700–2200 cm^{-1}) of the oxidative addition of CH_3I showed that the strong Rh(I)–carbonyl peak in the region of 1950–1990 cm^{-1} disappears with the simultaneous formation of a very low intensity Rh(III)–carbonyl peak at *c.* 2060 cm^{-1} and a strong Rh(III)–acyl peak at about 1720 cm^{-1}. This disappearance and simultaneous formation of these peaks (which not only demonstrate the presence but also give an indication of the relative concentration of the different species) is shown in the plot of absorbance versus time in Fig. 1.

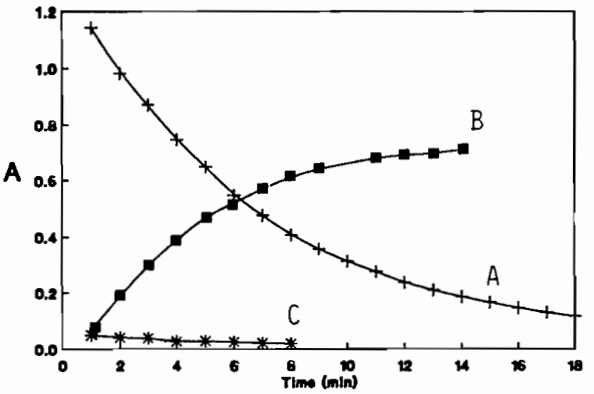

Fig. 1. Typical infrared time scans of the CO peaks for the oxidative addition of CH_3I to [Rh(Sacac)(CO)(PPh_3)] in 1,2-dichloroethane at 25 °C. A: Disappearance of [Rh(Sacac)-(CO)(PPh_3)] (ν(CO) = 1978 cm^{-1}), B: formation of acetyl peak (ν(CO) = 1720 cm^{-1}, C: disappearance of ionic intermediate (ν(CO) = 2060 cm^{-1}).

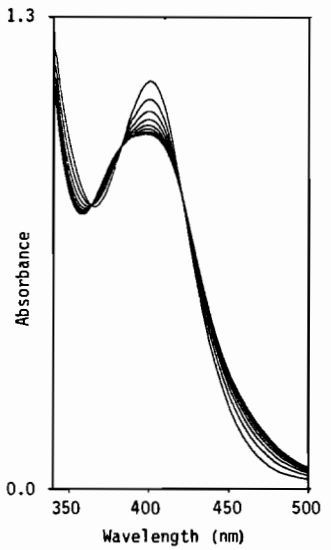

Fig. 2. Repetitive scans (2.5 min intervals) for the oxidative addition of CH_3I (0.5 M) to [Rh(Sacac)(CO)(PPh_3)] (2×10^{-4} M) in acetone at 25 °C.

It must be pointed out that the Rh(III)–CO peak at *c.* 2060 cm^{-1} is normally a high intensity peak as was for example found in the case of [Rh(acac)-(CO)(CH_3)(I)(PPh_3)] [2] and [Rh(cupf)(CO)(CH_3)-(I)(PPh_3)] [3]. The low intensity Rh(III)–CO peaks thus indicate that these species remain at a very low concentration during the reaction and that they are rapidly converted to the final acyl complexes with ν(CO) at about 1720 cm^{-1}. The smooth conversion of the Rh(I) complex to the Rh(III)–acyl complex is also seen in the UV–Vis time scans. Three isosbestic points (such as in Fig. 2) which remain throughout the reaction were observed for

TABLE 2. Isosbestic points in the reaction of [Rh(Sacac)(CO)(PX_3)] with CH_3I in acetone at 25 °C

X	Isosbestic points (nm)		
p-$CH_3OC_6H_4$	354	386	421
C_6H_5	360	381	421
p-ClC_6H_4	364	370	417
C_6H_{11}	358	389	445

the reaction of all the phosphine complexes. These isosbestic points are listed in Table 2.

According to these results the following reaction scheme may be presented:

$$[Rh(Sacac)(CO)(PX_3)] + CH_3I \quad \nu = 1960\text{–}1990\ cm^{-1}$$

$$k_1 \Big\| k_{-1}$$

$$Rh(III)\text{–}CO\ Complex \quad \nu = 2060\ cm^{-1}$$

$$k_2 \Big\| k_{-2}$$

$$[Rh(Sacac)(COCH_3)(I)(PX_3)] \quad \nu(CO) = 1720\ cm^{-1}$$

In this reaction scheme the value of k_{-2} must be small since the Rh(I) complex is completely converted to the final acyl complex even at a low concentration of CH_3I. The final complexes are also stable in solution and no conversion to the alkyl complex (as was found for the oxidative addition of CH_3I to [Rh(acac)(CO)(PPh_3)] was detected even after 400 times the half-lives of the reactions.

The plots of $\ln(|A_\infty - A_t|)$ versus time for the disappearance of the Rh(I)–CO peak as well as for the formation of the Rh(III)–acyl carbonyl peak were linear for at least two half-lives while the plots of the pseudo-first-order rate constants versus $[CH_3I]$ were linear with a zero intercept. The observed second-order rate constants (k_{obs}) as determined from these data at 25 °C are listed in Table 3. It is clear that the rate constants as determined from the disappearance of the Rh(I)–CO peak and the formation of the Rh(III)–acyl carbonyl peak are the same within experimental error.

The first three phosphine entries in Table 3 have the same cone angle θ [14] and thus the same stereochemical demand. They should however influence the Rh(I) centre differently as a result of the differences in the electronegativity of the substituent groups. The second-order rate constants show about a ten-fold increase from the P(p-$ClC_6H_4)_3$ to the P(p-$CH_3OC_6H_4)_3$ complex. This tendency is directly related to the σ-donor ordering of P(p-$CH_3OC_6H_4)_3 > PPh_3 >$ P(p-$ClC_6H_4)_3$ and thus the relative basicity of the Rh(I) complex. The carbonyl stretching vibrations (Table 1) which are a function of the electron density on the rhodium atom display the same dependence of the metal basicity on the σ-donor ability of the phosphine ligand. It is thus clear that an increased electron density on the Rh(I) centre leads to an increase in the reactivity of the complex towards oxidative addition reactions.

According to the electronic effect of the different phosphines it is expected that the rate constant for the P($C_6H_{11})_3$ complex should be larger than for the P(p-$CH_3OC_6H_4)_3$ complex. This would also be in agreement with the carbonyl wavenumbers of these complexes (see Table 1) which indicate the relative good σ-donocity of the P($C_6H_{11})_3$ ligand resulting in a strong Lewis base complex. The observed rate constant for the P($C_6H_{11})_3$ complex is however of the same order as that for the P(p-$ClC_6H_4)_3$ complex. The relative low reactivity of the P($C_6H_{11})_3$ complex may be ascribed to steric hindrance of the more bulky P($C_6H_{11})_3$ ligand with a cone angle of 165° in comparison with the cone angle of 145° for the other phosphines [14]. It is thus clear that electronic as well as steric influences are important in determining the reactivity of these complexes towards oxidative addition reactions.

It was possible to study the reactions by means of infrared spectrophotometry in only three solvents, i.e. 1,2-dichloroethane, acetone and ethylacetate. The reactions in the last two solvents could only be monitored in the 1950–2100 cm^{-1} region. The absorption of toluene and chlorobenzene is too high in the 1700–2100 cm^{-1} region while the solubility of [Rh(Sacac)(CO)(PPh_3)] in acetonitrile is too low. The reaction rate constants in these

TABLE 3. Rate constants and activation parameters for the oxidative addition of CH_3I to [Rh(Sacac)(CO)(PX_3)] complexes in 1,2-dichloroethane at 25.0 °C

X	k_{obs}[a] × 10^3 (M^{-1} s^{-1})	k_{obs}[b] × 10^3 (M^{-1} s^{-1})	$\Delta H^{\neq}$ (kJ mol^{-1})	$\Delta S^{\neq}$ (J mol^{-1} K^{-1})
p-$CH_3OC_6H_4$	11.9(3)	11.8(6)	39.4(12)	−150(6)
C_6H_5	5.52(8)	4.92(8)	46.5(30)	−134(11)
p-ClC_6H_4	1.10(5)	1.10(5)	47.3(17)	−143(7)
C_6H_{11}	1.74(8)			

[a]Rh(I)–CO peak data. [b]Rh(III)–acyl carbonyl peak data.

TABLE 4. Effect of the solvent on the reaction rate constant for the oxidative addition of CH_3I to [Rh(Sacac)(CO)(PPh_3)] at 25 °C

Solvent	k_{obs}[a] × 10^4 (M^{-1} s^{-1})	k_{obs} × 10^4 (M^{-1} s^{-1})	λ (nm)	ϵ[b]	D_n[b]	$\Delta H^{\neq}$ (kJ mol^{-1})	$\Delta S^{\neq}$ (J mol^{-1} K^{-1})
Toluene		2.17(4)	403	2.4		68.0(2)	−87(6)
Ethylacetate	5.86(8)	5.47(5)	403	6.0	17.1		
Chlorobenzene		8.36(6)	406	5.6			
Acetone	30.0(6)	30.1( )	397	20.7	17.0	50.7(9)	−122(3)
1,2-Dichloroethane	55.2(8)	56.0(7)	402	10.1	~0.1	46.5(30)	−134(11)
Acetonitrile		82.7(7)	325	36.1	14.1	47.0(20)	−128(7)

[a]From data at ν(CO) = 1978 cm^{-1}. [b]Ref. 15.

solvents were therefore determined by means of absorption measurements in the visible region. The plots of $\ln(A_\infty - A_t)$ versus time were also linear for at least two half-lives. The second-order rate constants were determined from plots of the pseudo first-order rate constants versus $[CH_3I]$ which were also linear with a zero intercept and are given in Table 4. It is clear that the rate constants as determined from the disappearance of the Rh(I)–CO peak at 1978 cm^{-1} are within the experimental error the same as those obtained from measurements in the visible region. A forty-fold variation of the rate constants was observed in the different solvents used.

The results in Table 4 indicate that the reaction rates are not dependent on the donicity of the solvent as in the case for the oxidative addition reactions of [Rh(cupf)(CO)(PPh_3)]. A solvent-assisted path was however observed for the latter reaction. The effect of the solvent on the reaction rate however clearly indicates a significant increase in the reactivity of [Rh(Sacac)(CO)(PPh_3)] in more polar solvents. This can be taken as evidence that the function of the solvent is to ease the charge separation during the formation of the transition state.

This evidence is in agreement with the observation that the volume of activation for the oxidative addition of CH_3I to a similar Rh(I) complex [Rh(cupf)(CO)(PPh_3)] is much more negative in the more polar solvent methanol than in acetone [5]. A polar transition state

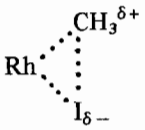

I

or $Rh^{\delta+}\cdots\cdots CH_3\cdots\cdots I^{\delta-}$

II

may thus accordingly be proposed.

If these reactions proceed via transition state II the observed intermediate with ν(CO) at about 2060 cm^{-1} may be formulated as the ionic intermediate [Rh(Sacac)(CO)(PPh_3)(CH_3)]$^+I^-$.

If transition state I (for a concerted three-centered mechanism) is assumed *cis*-addition of CH_3I should occur and the observed intermediate may be formulated as the neutral complex [Rh(Sacac)(CO)(PPh_3)(CH_3)(I)].

The crystal structure determination of [Rh(cupf)(CO)(PPh_3)(CH_3)(I)] indeed proved that *cis*-addition took place during the oxidative addition of CH_3I to [Rh(cupf)(CO)(PPh_3)].

According to the kinetic results and the possible transition states the following mechanisms may be proposed.

Transition state II

$$[Rh(Sacac)(CO)(PPh_3)] + CH_3I \xrightarrow{k_1 \text{ slow}} [Rh(Sacac)(CO)(PPh_3)(CH_3)]^+I^- \xrightarrow{k_2 \text{ fast}} [Rh(Sacac)(COCH_3)(PPh_3)(I)] \quad (1)$$

or

Transition state I

$$[Rh(Sacac)(CO)(PPh_3)] + CH_3I \xrightarrow{k_1 \text{ slow}} [Rh(Sacac)(CO)(PPh_3)(CH_3)(I)] \xrightarrow{k_2 \text{ fast}} [Rh(Sacac)(COCH_3)(PPh_3)(I)] \quad (2)$$

According to these reaction schemes the observed second-order rate constants, k_{obs}, are equal to k_1.

It may be noted that reaction (1) is essentially the same as the one proposed for the oxidative addition of CH_3I to the corresponding β-diketone complexes with the exception that no transformation from the Rh(III)–acyl complex to a final six-coordinated alkyl complex was detected in the present study [2]. The large negative values of $\Delta S^{\neq}$ however may be indicative of transition state I,

reaction (2). To distinguish between transition states I and II we plan a detailed high-pressure kinetic study. It is clear that the alkyl intermediate (whether a five- or six-coordinated species) is quite reactive since the rate of disappearance of the rhodium(I) complex is the same as the rate of formation of the rhodium(III)–acyl complex. This may be explained by the capability of Sacac (being a better nucleophile than β-diketones) to destabilize the rhodium(III)–alkyl bond.

Acknowledgements

We thank the South African C.S.I.R. and the research fund of this University for financial assistance.

References

1 S. S. Basson, J. G. Leipoldt and J. T. Nel, *Inorg. Chim. Acta, 84* (1984) 167.
2 S. S. Basson, J. G. Leipoldt, A. Roodt, J. A. Venter and T. J. van der Walt, *Inorg. Chim. Acta, 119* (1986) 35.
3 S. S. Basson, J. G. Leipoldt, A. Roodt and J. A. Venter, *Inorg. Chim. Acta, 128* (1987) 31.
4 G. J. van Zyl, G. J. Lamprecht, J. G. Leipoldt and T. W. Swaddle, *Inorg. Chim. Acta, 143* (1988) 223.
5 J. G. Leipoldt, E. C. Steynberg and R. van Eldik, *Inorg. Chem., 26* (1987) 3068.
6 C. E. Johnson and R. Eisenberg, *J. Am. Chem. Soc., 107* (1985) 3148.
7 J. F. Roth, J. H. Craddock, A. Hershman and F. E. Paulik, *Chem. Technol.*, (1971) 600.
8 Chien-Hong Cheng, Bruce D. Spivack and Richard Eisenberg, *J. Am. Chem. Soc., 99* (1977) 3003.
9 J. G. Leipoldt, to be published.
10 S. S. Basson, J. G. Leipoldt, A. Roodt and J. A. Venter, *Inorg. Chim. Acta, 118* (1986) 445.
11 F. Duns and J. W. Anthonsen, *Acta Chem. Scand., Ser. B, 31* (1977) 40.
12 F. Duns, *J. Am. Chem. Soc., 108* (1986) 630.
13 L. J. Botha, S. S. Basson and J. G. Leipoldt, *Inorg. Chim. Acta, 126* (1987) 25.
14 C. A. Tolman, *Chem. Rev., 77* (1977) 313.
15 U. Mayer and V. Gutmann, *Adv. Inorg. Chem. Radiochem., 17* (1975) 189.